Orbital-based Scenario for Magnetic Structure of Neptunium Compounds

Hiroaki Onishi and Takashi Hotta

Advanced Science Research Center, Japan Atomic Energy Research Institute, Tokai, Ibaraki 319-1195, Japan

Abstract. In order to understand a crucial role of orbital degree of freedom in the magnetic structure of recently synthesized neptunium compounds $NpTGa_5$ (T=Fe, Co, and Ni), we propose to discuss the magnetic phase of an effective two-orbital model, which has been constructed based on a j-j coupling scheme to explain the magnetic structure of uranium compounds $UTGa_5$. By analyzing the model with the use of numerical technique such as exact diagonalization, we obtain the phase diagram including several kinds of magnetic states. An orbital-based scenario is discussed to understand the change in the magnetic structure among C-, A-, and G-type antiferromagnetic phases, experimentally observed in $NpFeGa_5$, $NpCoGa_5$, and $NpNiGa_5$.

1. Introduction

Recently it has been widely recognized that orbital degree of freedom plays an essential role for the understanding of novel magnetism in transition metal oxides [1]. A typical material is manganese oxide, exhibiting remarkable colossal magneto-resistance phenomena [2]. Due to competition and interplay among spin, charge, and orbital degrees of freedom, rich phase diagram has been revealed [1], but a recent trend is to unveil further new phases both from experimental and theoretical investigations. In fact, even in undoped $RMnO_3$ (R=rare earth lanthanide ions), a novel antiferromagnetic (AF) phase called the "E-type" spin structure has been reported as the ground state for R=Ho [3, 4]. Here we follow the definitions of spin structure in Ref. [5]. The origin of the E-AF phase has been clarified theoretically [6] based on a band-insulator scenario in the e_g-orbital systems [7, 8, 9]. It should be noted that the ground state of undoped manganites was just considered to be well understood, since for most R-ions, the A-type AF insulating phase appears with the C-type ordering of the $(3x^2-r^2)$- and $(3y^2-r^2)$- orbitals [10, 11, 12, 13, 14, 15, 16, 17, 18, 19, 20, 21, 22, 23, 24]. Moreover, also for the half-doped manganite $La_{0.5}Ca_{0.5}MnO_3$, a charge-ordered ferromagnetic (FM) phase has been found in experiments [25, 26], as predicted theoretically [27, 28]. These facts clearly indicate the importance of both experimental and theoretical efforts to unveil new phases in manganites in addition to the explanation of the complex phases already observed. Such efforts have also been made to find new phases in other transition metal oxides, for instance, ruthenates [29, 30] and nickelates [31].

A trend to seek for new magnetic as well as superconducting phases has been also found in the f-electron system, which is another type of spin-charge-orbital complex. Among many kinds of f-electron materials, in recent years, f-electron compounds with $HoCoGa_5$-type tetragonal crystal structure [see Fig. 1(a)], frequently referred to as "115", have been intensively investigated both in experimental and theoretical research fields of condensed matter physics. Such vigorous activities are certainly motivated by high superconducting transition temperature T_c observed in some 115 compounds. Especially, amazingly high value of T_c=18.5K has been reported in $PuCoGa_5$ [32, 33, 34] and the mechanism has been discussed theoretically [35, 36]. Among 115 compounds, interesting magnetic properties have been reported for $UTGa_5$, where T is a transition metal ion [37, 38, 39, 40, 41, 42, 43, 44, 45, 46, 47, 48]. In particular, neutron scattering experiments have revealed that $UNiGa_5$ exhibits the G-type AF phase, while $UPdGa_5$ and $UPtGa_5$ have the A-type AF state [44, 48]. Note that G-type indicates a three-dimensional Néel state, while A-type denotes a layered AF structure in which spins align ferromagnetically in the ab plane and AF along the c axis [5]. It is quite interesting that the magnetic structure is different for U-115 compounds which differ only by the substitution of transition metal ions.

Quite recently, 115 compounds including neptunium have been skillfully synthesized and several kinds of physical quantities have been successfully measured [49, 50, 51, 52, 53, 54, 55, 56]. Especially, the de Haas-van Alphen (dHvA) effect has been observed in
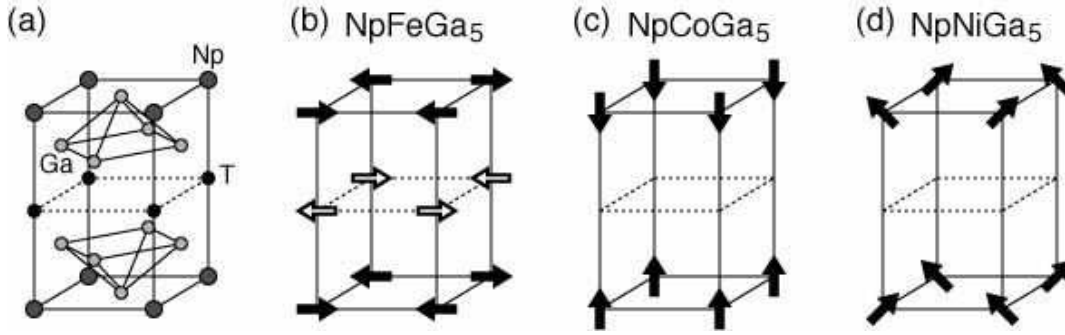
Figure 1. (a) Crystal structure of $NpTGa_5$. Schematic views of magnetic structures composed of magnetic moments of Np ions for (b) $NpFeGa_5$, (c) $NpCoGa_5$, and (d) $NpNiGa_5$. For $NpFeGa_5$, magnetic moments at Fe sites are also depicted.

$NpNiGa_5$ [50], which is the first observation of dHvA signal in transuranium compounds. For $NpCoGa_5$, the dHvA oscillations have been also detected and a couple of cylindrical Fermi surfaces are found [52]. For $NpFeGa_5$, the magnetic moment at Fe site has been suggested in neutron scattering experiments [56] and it has been also detected by ^{57}Fe Mössbauer spectroscopy [55]. Interestingly enough, the magnetic structure of Np-115 compounds also depends sensitively on transition metal ion [53, 56]: C-AF for $NpFeGa_5$, A-AF for $NpCoGa_5$, and G-AF for $NpNiGa_5$, as shown in Figs. 1(b)-(d). Note that for $NpNiGa_5$, the G-AF structure is composed of canted Np moments and the peak in the neutron scattering intensity grows *after* the FM transition occurs [53, 56]. In any case, it is characteristic of U-115 and Np-115 compounds that the magnetic properties are sensitive to the choice of transition metal ions.

The appearance of several kinds of AF states reminds us of the magnetic phase diagram of manganites and thus, we envisage a scenario to understand the complex magnetic structure of actinide compounds based on an orbital degenerate model similar to that of manganites. However, one must pay close attention to the meanings of "spin" and "orbital" in f-electron systems. Since they are tightly coupled with each other through a strong spin-orbit interaction, distinguishing them is not straightforward in comparison with d-electron systems. This point can create serious problems when we attempt to understand microscopic aspects of magnetism and superconductivity in f-electron compounds. Thus, it is necessary to carefully define the terms "orbital" and "spin" for f electrons in a microscopic discussion of magnetism and superconductivity in actinide compounds.

In order to overcome such problems, we have proposed to employ a j-j coupling scheme to discuss f-electron systems [35]. Here we stress the advantages of the j-j coupling scheme. First, it is quite convenient for the inclusion of many-body effects using standard quantum-field theoretical techniques, since individual f-electron states are clearly defined. In contrast, in the LS coupling scheme we cannot use such standard techniques, since Wick's theorem does not hold. Second we can, in principle, include the effects of valence fluctuations. In some uranium compounds, the valence of the

uranium ion is neither definitely U^{3+} nor U^{4+}, indicating that the f-electron number takes a value between 2 and 3. In the j-j coupling scheme this is simply regarded as the average number of f electron per uranium ion.

In this paper, we attempt to explain the complex magnetic structure of Np-115 based on the effective two-orbital model, which has been constructed from the j-j coupling scheme in order to understand the magnetic properties of U-115 compounds [57]. We depict the Fermi surfaces of the kinetic term of $5f$ electron based on the j-j coupling scheme in comparison with those obtained from the dHvA experiments. The agreement seems to be fairly well, but the present itinerant picture should be critically discussed. Then, we apply the exact diagonalization technique to the model in a small $2\times2\times2$ cube to obtain a clue to understand the complex magnetic structure of NpTGa$_5$. The phase diagrams are found to include G-, A-, and C-type AF states, consistent with experimental observations in Np-115.

The organization of this paper is as follows. In Sec. 2, we will introduce an effective Hamiltonian, called the Γ_8 model, for actinide 115 systems. In Sec. 3, we show the calculated results of the model Hamiltonian. The Fermi-surface structure is discussed in comparison with dHvA experimental results. We show numerical results for the magnetic structure obtained by using exact diagonalization technique. Finally, in Sec. 4, future developments are discussed and the paper is summarized. Throughout the paper, we use units such that $\hbar=k_{\mathrm{B}}=1$.

2. Model Hamiltonian

In this section, we show an effective model based on the j-j coupling scheme for Np-115 compounds, which is the same as the model for U-115 [57]. We emphasize that the model with orbital degree of freedom is applicable to actinide 115 materials in common.

2.1. Local f-electron state

In order to construct a microscopic Hamiltonian for f-electron systems, it is necessary to include simultaneously the itinerant nature of f electrons as well as strong electron correlation and the effect of crystalline electric field (CEF). For the purpose, we have proposed to use the so-called j-j coupling scheme [35]. As shown in Fig. 2, we include the spin-orbit coupling so as to define the state labeled by the total angular momentum. For f orbitals with $\ell=3$, we immediately obtain an octet with $j=7/2(=3+1/2)$ and a sextet with $j=5/2(=3-1/2)$, which are well separated by the spin-orbit interaction. In general, the spin-orbital coupling is as large as 1eV in actinide elements and thus, in the j-j coupling scheme, we consider only the $j=5/2$ sextet.

In actual compounds, due to the electrostatic potential from ligand ions surrounding the actinide ion, the six-fold degeneracy of $j=5/2$ is lifted, as shown in Fig. 2. Note that in the j-j coupling scheme, it is enough to define the one-electron potential, which is deduced from the CEF level scheme of corresponding f^1-electron system. First
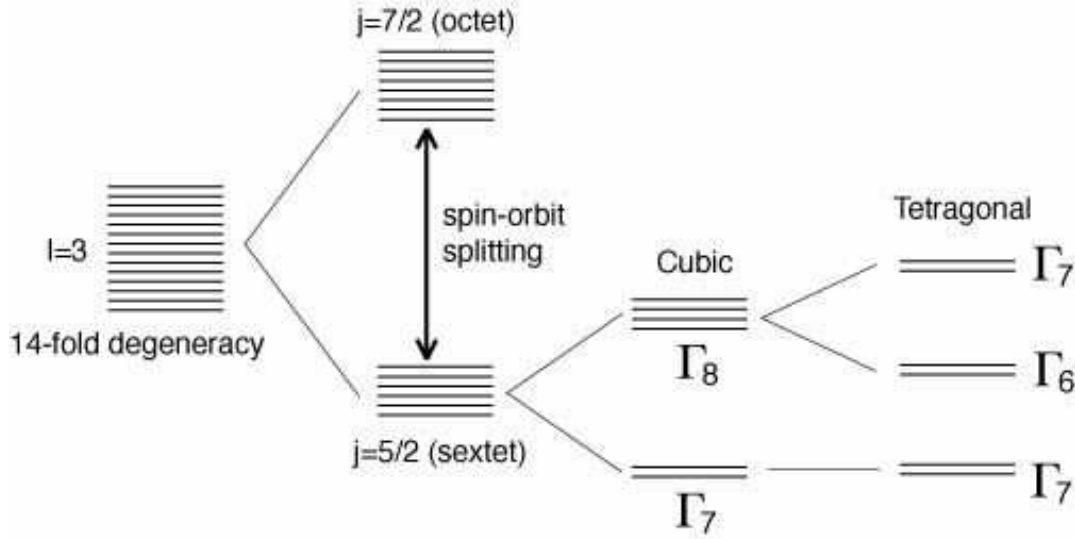
Figure 2. Schematic view for local f-electron state in the j-j coupling scheme. The $j=5/2$ sextet is split into several Kramers doublets due to cubic or tetragonal crystalline electric field effect.

we consider the one f-electron state in the $AuCu_3$-type cubic crystal structure, since this is the mother structure of $HoCoGa_5$-type tetragonal compound. The effects of tetragonality will be discussed later. For the case of cubic symmetry, we identify two eigen energies as $-240B_4^0$ for the Γ_7 doublet and $120B_4^0$ for the Γ_8 quartet, where B_4^0 is a cubic CEF parameter. For the following discussion, it is quite convenient to introduce "pseudospin" to distinguish the degenerate states of the Kramers doublet and "orbital" to label the different Kramers doublets in Γ_8 quartet. In Fig. 3(a), we show the shape of the wavefuction of two Γ_8 orbitals, Γ_8^a and Γ_8^b.

In order to proceed with the discussion, we need to know which is lower, Γ_7 or Γ_8, in the one f-electron picture. For some crystal structures, it is possible to determine the level scheme from intuitive discussions on f-electron wavefunctions and the positions of ligand ions. However, this is not the case for the $AuCu_3$-type crystal structure. For this case we invoke certain experimental results on $CeIn_3$, a typical $AuCu_3$-type Ce-based compound, where Γ_7 and Γ_8 have been reported as ground and excited states, respectively, with an energy difference of 12meV [58]. Thus, we take Γ_7 to be lower for the present considerations, as shown in Fig. 3(b).

In the j-j coupling scheme for UGa_3 and $NpGa_3$, it is necessary to accommodate three or four electrons in the one-electron energy states Γ_7 and Γ_8. We immediately notice that there are two possibilities, i.e., low- and high-spin states, depending on the Hund's rule interaction and the splitting between the Γ_7 and Γ_8 levels. As discussed in Ref. [35], the effective Hund's rule interaction becomes small in the j-j coupling scheme and thus, the low-spin state should be realized, as shown in Figs. 3(c) and (d). We emphasize that the low-spin state is consistent with the LS coupling scheme. In the electron configuration shown in Figs. 3(c) and (d), the Γ_7 level is fully occupied to form
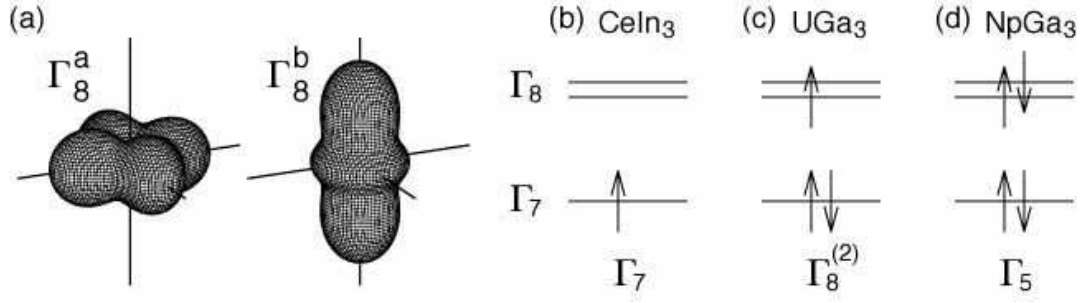
Figure 3. (a) Two orbitals, a and b, in the Γ_8 model. Level scheme for (b) CeIn$_3$, (c) UGa$_3$, and (d) NpGa$_3$ based on the j-j coupling scheme. Here we assume trivalent actinide ions as U^{3+} ($5f^3$) and Np^{3+} ($5f^4$). It should be noted that up and down arrows denote pseudospins to distinguish the states in the Kramers doublet. Note also that for NpGa$_3$, a couple of electrons in Γ_8 orbitals form a local triplet, leading to Γ_5.

a singlet. If this Γ_7 level is located well below the Γ_8, the occupying electrons will not contribute to the magnetic properties. Thus, we ignore the Γ_7 electrons in the following discussion. As for details to validate the suppression of Γ_7 level, readers should refer Ref. [57]. We also mention another theoretical effort based on the j-j coupling scheme, in which the dual nature, itinerant and localized, of $5f$ electron has been emphasized [59, 60, 61].

As shown in Fig. 1(a), since 115 compounds have the tetragonal structure, we need to include the effect of tetragonality. In the tetragonal structure, the quartet Γ_8 is further split into two doublets, Γ_6 and Γ_7, as shown in Fig. 2. Namely, there appear three Kramers doublets with one Γ_6 and two Γ_7. Note that two Γ_7 states are obtained from the mixture of Γ_7 and Γ_8^a in the cubic symmetry. However, for simplicity, we ignore the change of wavefunctions from cubic to tetragonal systems, since we believe that the existence of orbital degree of freedom is a key issue to understand the complex magnetic structure of actinide compound. For the purpose to improve the present theory from the quantitative viewpoint, it may be important to include also the deformation of local f-electron wavefunction, but we postpone such a study in the future. In this paper, we consider the splitting energy between Γ_8 orbitals, in order to take into account the tetragonality in the 115 compounds.

2.2. Γ_8 model

After tedious calculations, we obtain the Hamiltonian including Γ_8 orbitals in the form of [35, 57]

$$H = H_{\mathrm{kin}} + H_{\mathrm{CEF}} + H_{\mathrm{C}}, \tag{1}$$

where H_{kin} denotes the kinetic term of $5f$ electrons, H_{CEF} is the CEF potential term, and H_{C} indicates the Coulomb interaction term among Γ_8 electrons.

Concerning the kinetic term, one traditional way is to consider the hybridization process between f and conduction electrons. For 115 systems, from the band-structure

calculations [36], p electrons of Ga ion play an important role to form conduction band. However, based upon a picture that $5f$ electrons are itinerant, we can consider another way to construct the kinetic term for f electrons within a tight-binding approximation. In actual compounds, there should occur several processes through other ligand ions, in addition to the direct process of f electrons. However, when we include correctly the local symmetry of relevant f orbitals, it is believed that we can grasp qualitative point of kinetic term of f electrons, even within the simple tight-binding approximation. This point will be discussed elsewhere in future. Here we do not consider the hybridization process. Then, the kinetic term is given in the tight-binding approximation for f electrons as

$$H_{\text{kin}} = \sum_{\mathbf{i},\mathbf{a},\sigma,\tau,\tau'} t^{\mathbf{a}}_{\tau\tau'} f^{\dagger}_{\mathbf{i}\tau\sigma} f_{\mathbf{i}+\mathbf{a}\tau'\sigma}, \tag{2}$$

where $f_{\mathbf{i}\tau\sigma}$ is the annihilation operator for an f electron with pseudospin σ in the τ-orbital at site $\mathbf{i}$ and $t^{\mathbf{a}}_{\tau\tau'}$ is the f-electron hopping matrix element between τ- and τ'-orbitals along the $\mathbf{a}$ direction. Indices a and b denote the Γ_8^a and Γ_8^b orbitals, respectively. In the xy plane and along the z-axis, $t^{\mathbf{a}}_{\tau\tau'}$ is given by

$$t^{\mathbf{x}}_{\tau\tau'} = t \begin{pmatrix} 3/4 & -\sqrt{3}/4 \\ -\sqrt{3}/4 & 1/4 \end{pmatrix}, \tag{3}$$

for the $\mathbf{x}$-direction,

$$t^{\mathbf{y}}_{\tau\tau'} = t \begin{pmatrix} 3/4 & \sqrt{3}/4 \\ \sqrt{3}/4 & 1/4 \end{pmatrix}, \tag{4}$$

for the $\mathbf{y}$ direction, and

$$t^{\mathbf{z}}_{\tau\tau'} = \begin{pmatrix} 0 & 0 \\ 0 & t^{\mathbf{z}}_{bb} \end{pmatrix}, \tag{5}$$

for the $\mathbf{z}$ direction. Note that $t=(3/7)(ff\sigma)$, where $(ff\sigma)$ is a Slater-Koster overlap integral between f orbitals through σ bond. In the following, t is taken as an energy unity. Remark that we introduce another hopping amplitude along the z-axis. In AnTGa$_5$ (An=U and Np), AnGa$_2$ layer is sandwiched by two AnGa$_3$ sheets, indicating that the hopping of f electron along the z-axis should be reduced from that in AnGa$_3$. However, it is difficult to estimate the reduction quantitatively, since it is necessary to include correctly the hybridization with d electrons in transition metal ions and p electrons in Ga ions. Thus, in this paper, we consider the effective reduction by simply treating $t^{\mathbf{z}}_{bb}$ as a parameter. For a practical purpose, we introduce a non-dimensional parameter $t_z = t^{\mathbf{z}}_{bb}/t$.

We point out that the hopping amplitudes among Γ_8 orbitals are just the same as those for the e_{g} orbitals of $3d$ electrons [1, 9]. Readers can intuitively understand this point from the shapes of Γ_8 orbitals shown in Fig. 3(a), which are similar to e_{g} orbitals. Mathematically, this is quite natural, if we recall the fact that Γ_8 is isomorphic to $\Gamma_3 \times \Gamma_6$, where Γ_3 indicates E representation for the orbital part and Γ_6 denotes the spin part.

Note, however, that the agreement between f- and d-electron hopping amplitudes is due to the choice of special axis directions. If we take the (1,1,0) direction in an fcc lattice, f-electron hopping amplitude becomes complex, leading to the stabilization of octupole ordering in NpO_2 [62].

The CEF term is given by

$$H_{\mathrm{CEF}} = -\Delta \sum_{\mathbf{i}} (\rho_{\mathbf{i}a} - \rho_{\mathbf{i}b})/2, \tag{6}$$

where $\rho_{\mathbf{i}\tau\sigma} = f^{\dagger}_{\mathbf{i}\tau\sigma} f_{\mathbf{i}\tau\sigma}$, $\rho_{\mathbf{i}\tau} = \sum_{\sigma} \rho_{\mathbf{i}\sigma\tau}$, and Δ is the level splitting, which expresses the effect of tetragonal CEF, as discussed above. We note that in actuality, Δ should be related to the value of t_z, since both quantities depend on the lattice constant along the z axis. However, the relation between t_z and Δ is out of the scope of this paper and thus, here we simply treat them as independent parameters.

The Coulomb interaction term is expressed by

$$H_{\mathrm{C}} = U \sum_{\mathbf{i},\tau} \rho_{\mathbf{i}\tau\uparrow}\rho_{\mathbf{i}\tau\downarrow} + U' \sum_{\mathbf{i}} \rho_{\mathbf{i}a}\rho_{\mathbf{i}b}$$
$$+ J \sum_{\mathbf{i},\sigma,\sigma'} f^{\dagger}_{\mathbf{i}a\sigma} f^{\dagger}_{\mathbf{i}b\sigma'} f_{\mathbf{i}a\sigma'} f_{\mathbf{i}b\sigma} + J' \sum_{\mathbf{i},\tau\neq\tau'} f^{\dagger}_{\mathbf{i}\tau\uparrow} f^{\dagger}_{\mathbf{i}\tau\downarrow} f_{\mathbf{i}\tau'\downarrow} f_{\mathbf{i}\tau'\uparrow}, \tag{7}$$

where the Coulomb interactions U, U', J, and J' denote intra-orbital, inter-orbital, exchange, and pair-hopping interactions among Γ_8 electrons, respectively, expressed by using the Racah parameters [63]. Note that the relation $U=U'+J+J'$ holds, ensuring rotational invariance in pseudo-orbital space for the interaction part. For d-electron systems, one also has the relation $J=J'$. When the electronic wavefunction is real, this relation is easily demonstrated from the definition of the Coulomb integral. However, in the j-j coupling scheme the wavefunction is complex, and J is not equal to J' in general. For simplicity, we shall assume here that $J=J'$, noting that essential results are not affected. Since double occupancy of the same orbital is suppressed owing to the large value of U, pair-hopping processes are irrelevant in the present case.

3. Results

Now let us show our calculated results based on the two-orbital model. First we discuss the electronic properties of H_{kin} in the non-interacting limit by focusing on the Fermi-surface structure, in order to gain an insight into the interpretation of dHvA experiments on Np-115 compounds. Next the magnetic properties are discussed. We attempt to understand the appearance of three kinds of magnetic phases based on the orbital-based scenario similar to that of manganites.

3.1. Fermi-Surface Structure

Let us consider the structure of Fermi-surface sheets of the Γ_8 tight-binding model H_{kin}. In the following, we define n as the number of f electrons included in the Γ_8 state. Namely, the local f-electron number per actinide ion is $n+2$, by adding Γ_7 electrons.
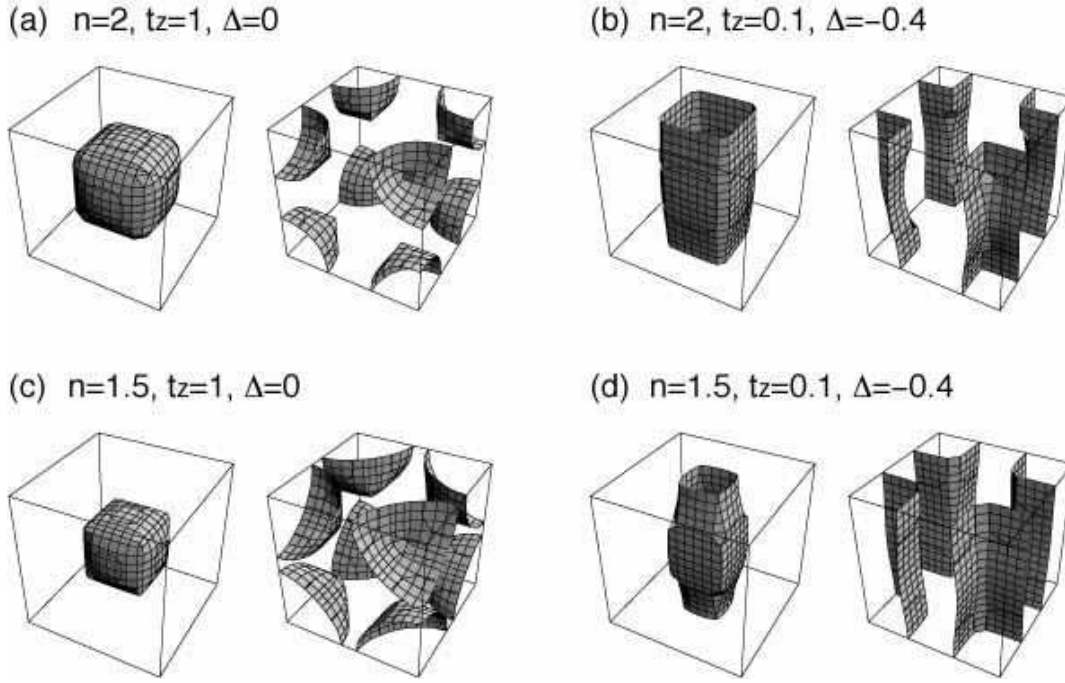
Figure 4. Fermi-surface sheets of the Γ_8 tight-binding model for (a) n=2, t_z=1, Δ=0, (b) n=2, t_z=0.1, Δ=−0.4, (c) n=1.5, t_z=1, Δ=0, and (d) n=1.5, t_z=0.1, Δ=−0.4. The bounding box indicates the first Brillouin zone for a simple cubic lattice. The Γ point is located at the center of the box, while the apices denote R points.

As shown in Fig. 3(d), in our picture, there are two Γ_8 electrons in trivalent neptunium ion. Then, it is quite natural to consider first the case of n=2. The results for (t_z, Δ)=(1,0) and (0.1,−0.4) are shown in Figs. 4(a) and (b), respectively. For the cubic case with t_z=1 and Δ=0, there exist two kinds of cube-like Fermi surfaces. One is centered at Γ point, while the center of another cube is R point. When we change t_z and Δ to consider the tetragonality, cubes gradually change to cylinders. As shown in Fig. 4(b), we can clearly observe two kinds of cylindrical Fermi surfaces. Note that the Fermi-surface structure does not sensitively depend on the value of Δ, as long as the absolute value is not so large as $|\Delta|$<0.5. It is important to have quasi orbital degeneracy, to reproduce a couple of cylindrical Fermi surfaces.

It is interesting to recall the dHvA experiment on $NpCoGa_5$, which has revealed two kinds of cylindrical Fermi surface [52]. In the relativistic band-structure calculations for the paramagnetic phase, it has been difficult to understand the appearance of a couple of cylindrical Fermi surfaces [36]. Note that the folding of the magnetic Brillouin zone cannot explain the discrepancy between the experimental results and the band-calculation ones for $NpCoGa_5$. A direct way to understand the dHvA experimental results is to improve the band-structure calculation method, but as shown in Fig. 4(b), even in a simple tight-binding model for itinerant $5f$ electrons, we obtain two kinds of cylindrical Fermi surface due to the effect of Γ_8 orbital degree of freedom. We do not claim that the dHvA results can be understood only by the present simple calculations,

but a hint to understand the electronic structure of Np-115 is believed to be hidden in the construction of our model with Γ_8 orbital degree of freedom.

We point out that in actual Np-115 compounds, the number of n is not definitely determined. Especially, due to the change of transition metal ion, the number of n seems to be changed effectively. In fact, in the relation between superconducting transition temperature T_c and the ratio of lattice constants c/a, the curve of T_c vs. c/a for solid solution (U,Np,Pu)CoGa$_5$ is similar to that for another solid solution Pu(Fe,Co,Ni)Ga$_5$ [64, 65]. Namely, in actinide 115 materials, the effect of the change of f-electron number due to the substitution of actinide ion seems to be similar to that of the substitution of transition metal ion. Thus, when we consider the change of the magnetic structure among NpTGa$_5$ (T=Fe, Co, and Ni) based on the effective two-orbital model, there is no strong reason to fix firmly $n=2$.

In Figs. 4(c) and (d), we show the Fermi-surface sheets for $n=1.5$, in which the number of f electrons is slightly decreased. We can observe that the Fermi-surface structure is not changed so much, although the cylinder centered at the Γ point becomes slender. Thus, as long as we are based on the simple tight-binding model, it is concluded that the structure of the Fermi-surface sheets is not changed sensitively by the number of n around at $n=2$. This result suggests that it is possible to change the value of n to consider the magnteic structure of Np-115 compounds.

3.2. Magnetic structure

Now we consider the magnetic properties of the Γ_8 model. Among several methods to analyze the microscopic model, in this paper we resort to an exact diagonalization technique on a 2×2×2 lattice. Although there is a demerit that it is difficult to enlarge the system size, we take a clear advantage that it is possible to deduce the magnetic structure by including the effect of electron correlation. In order to discuss the ground-state properties, it is useful to measure the spin and orbital correlations, which are, respectively, defined by

$$S(\boldsymbol{q}) = (1/N)\sum_{\mathbf{i},\mathbf{j}}\langle\sigma_{\mathbf{i}}^z\sigma_{\mathbf{j}}^z\rangle e^{i\boldsymbol{q}\cdot(\mathbf{i}-\mathbf{j})}, \tag{8}$$

with $\sigma_{\mathbf{i}}^z=\sum_\tau(n_{\mathbf{i}\tau\uparrow}-n_{\mathbf{i}\tau\downarrow})/2$, and

$$T(\boldsymbol{q}) = (1/N)\sum_{\mathbf{i},\mathbf{j}}\langle\tau_{\mathbf{i}}^z\tau_{\mathbf{j}}^z\rangle e^{i\boldsymbol{q}\cdot(\mathbf{i}-\mathbf{j})}, \tag{9}$$

with $\tau_{\mathbf{i}}^z=\sum_\sigma(n_{\mathbf{i}a\sigma}-n_{\mathbf{i}b\sigma})/2$. Here N is the number of sites.

First let us consider the case of $n=2$, which is corresponding to the trivalent Np ion. In Fig. 5(a), we show the spin correlation as a function of Δ for $U'=5$, $J=0$, and $t_z=1$. At $t_z=1$ and $\Delta=0$ (cubic system), local triplet composed of a couple of f electrons is formed at each site and the G-type AF structure is stabilized due to the so-called superexchange interaction. As easily observed, even when Δ is introduced as the tetragonal CEF effect, the G-AF structure remains robust for $|\Delta| < 1$. When $|\Delta|$ is larger than unity, two electrons simultaneously occupy the lower orbital, leading to the
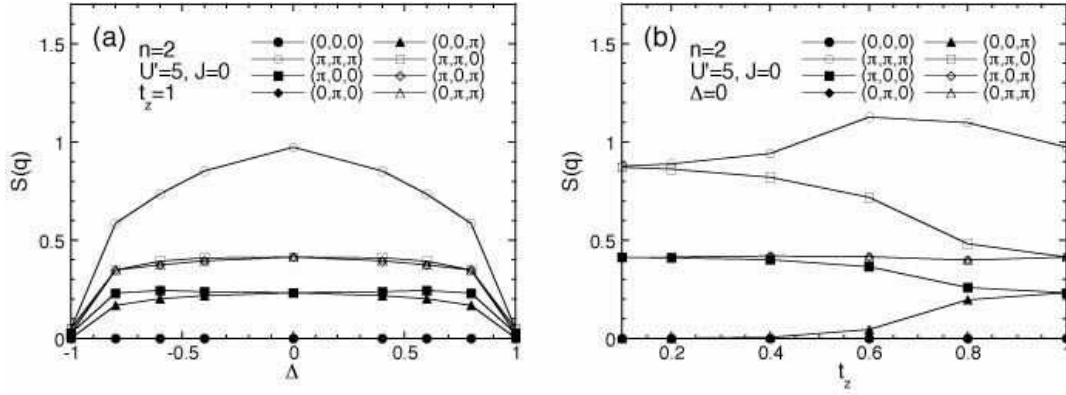
Figure 5. Spin correlation for $n=2$, $U'=5$, and $J=0$ as a function of (a) Δ for $t_z=1$ and of (b) t_z for $\Delta=0$.

non-magnetic state composed of local Γ_1, irrelevant to the present study to consider the magnetic phase. In Fig. 5(b), the spin correlation is shown as a function of t_z for $\Delta=0$. Again, the G-type AF structure is stabilized, but we find that the spin correlation of $\boldsymbol{q}=(\pi,\pi,0)$ comes to be equivalent to that of $\boldsymbol{q}=(\pi,\pi,\pi)$ with the decrease of t_z, since the AF structure is stabilized in each xy plane due to superexchange interaction and the planes are decoupled for small t_z.

At the first glance, it seems difficult to understand the variety of magnetic phases observed in NpTGa$_5$, when we consider only the trivalent Np ion. However, there is no *a priori* reason to fix the valence as Np^{3+}, as mentioned in the previous subsection. In NpTGa$_5$, d-electron band originating from transition metal ions may significantly affect the valence of Np ion. In addition, we also stress that the actual compounds exhibit AF metallic behavior. In the band-structure calculation, the average number of f electrons at Np ion is easily decreased from four. Thus, we treat the local f-electron number as a parameter.

We may consider another reason to decrease effectively the number of f electron from $n=2$ in NpGa$_3$. In the present two-orbital model, the G-AF structure is robust, which is natural from the theoretical viewpoint within the model. However, in the experimental result on NpGa$_3$, the low-temperature ground state is ferromagnetic, although the AF phase has been observed around at $T\sim60$K [66]. In order to understand the occurrence of the FM phase in the two-orbital model, it is necessary to inject some amount of "hole" in the AF phase, since the double-exchange mechanism works to maximize the kinetic motion of electrons, as will be discussed later in the main text. It is difficult to determine the amount of doped holes to obtain the FM phase, but at least qualitatively, the effective decrease of n seems to be physically meaningful in NpGa$_3$ as well as in NpTGa$_5$.

Now we consider the case of $n=1.5$. As discussed in the previous subsection, the Fermi-surface structure does not change so much from that of the case of $n=2$, when $|\Delta|$ is not so large. In Fig. 6(a), we show the ground-state phase diagram in the (U', J)
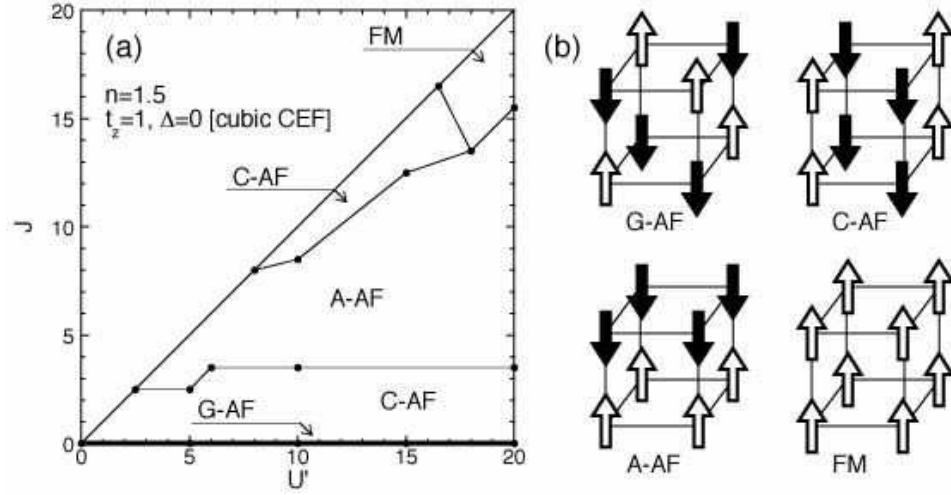
Figure 6. (a) Ground-state phase diagram in the (U', J) plane for $n=1.5$, $t_z=1$, and $\Delta=0$. (b) Spin structures in the G-type AF, C-type AF, A-type AF, and FM phases.

plane at $n=1.5$ for the cubic case with $t_z=1$ and $\Delta=0$. At $J=0$, a G-type AF structure is stabilized due to superexchange interaction in the same way as the case of $n=2$. However, the G-AF structure is immediately changed to a C-AF structure only by a small value of the Hund's rule interaction. With increasing J, the magnetic phase changes in the order of G-AF, C-AF, A-AF, and FM phases, except for the C-AF phase in the large J region. The spin structure of each phase is shown in Fig. 6(b). This result is quite natural, since we are now considering the magnetic structure based on the two-orbital model, in which the FM tendency is due to the optimization of kinetic motion of electrons.

In order to understand the underlying mechanism of the appearance of various magnetic structures in addition to the G-AF structure for $n=1.5$, we consider the case of $J=0$. In Fig. 7(a), we show typical results of the spin correlation as a function of Δ for $U'=5$, $J=0$, and $t_z=1$. At $\Delta=0$, the dominant component of $S(\boldsymbol{q})$ appears at $\boldsymbol{q}=(\pi, \pi, \pi)$, indicating the G-type AF structure. On the other hand, in the region of positive small Δ, the spin correlation of $\boldsymbol{q}=(\pi, \pi, 0)$ turns to be dominant, indicating the C-type AF structure. This phase is defined as C-AF(I). Concerning the orbital correlation, we find no remarkable structure in the C-AF(I) phase, as shown in Fig. 7(b). Note that in the G-AF phase with positive Δ, the orbital correlation of $\boldsymbol{q}=(0,0,0)$ has a significant value in comparison with other regions, since electrons tend to doubly occupy lower Γ_8^a orbitals. This G-AF phase is called G-AF(I). On the other hand, in the G-AF phase with negative Δ, there is no indication of the development of the orbital correlation of $\boldsymbol{q}=(0,0,0)$, since the lower Γ_8^b orbitals are singly occupied. We label this G-AF phase as G-AF(II) to distinguish it from G-AF(I). It is interesting to see different types of the G-AF phases due to the change of the orbital state.
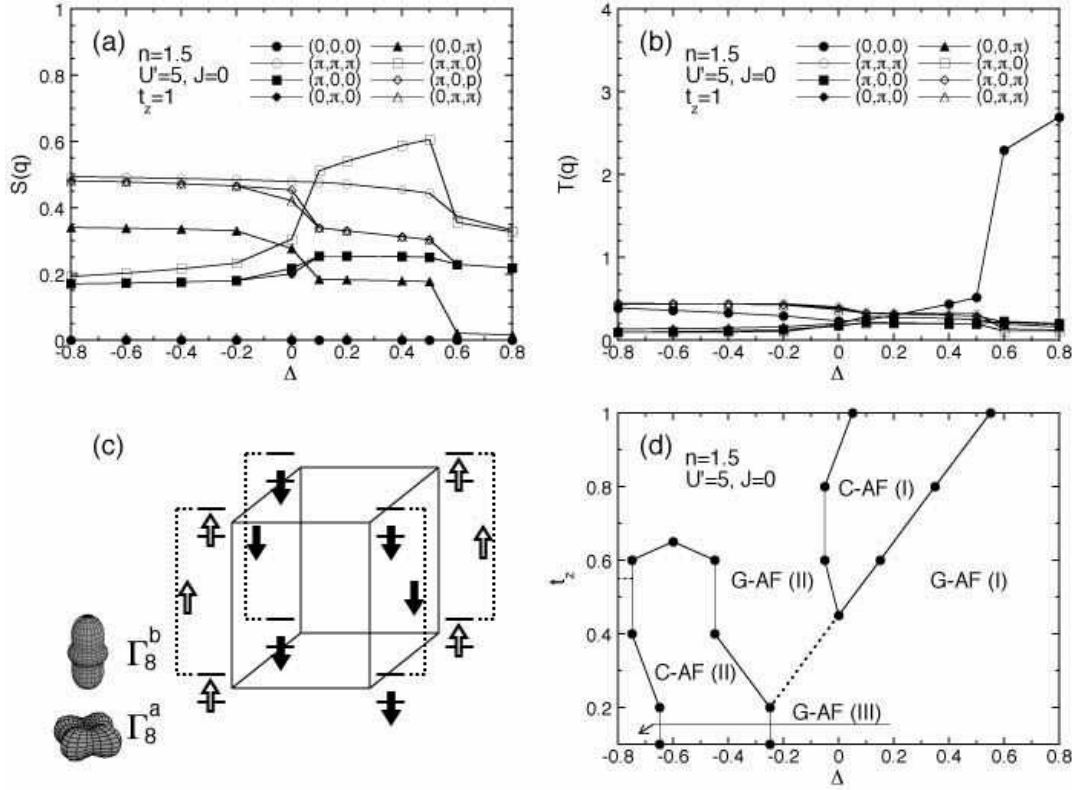
Figure 7. (a) Spin and (b) orbital correlations as a function of Δ for $n=1.5$, $U'=5$ $J=0$, and $t_z=1$. (c) Schematic view of the electron configuration in the C-AF phase in the region near $t_z=1$. (d) Ground-state phase diagram of the magnetic structure in the (Δ, t_z) plane.

Let us now discuss the reason of the appearance of the C-AF(I) phase in the region of positive small Δ. For $\Delta>0$, the energy level of Γ_8^a is lower than that of Γ_8^b by definition. Then, the Γ_8^a orbital is first occupied by one electron at each site. The rest of electrons are accommodated in Γ_8^b orbitals to avoid the effect of intra-orbital Coulomb interaction when Δ is not large so much. The electrons in Γ_8^a orbitals hop to the Γ_8^a orbital at the nearest-neighbor site, since the Γ_8^b has higher energy. Since the electrons in Γ_8^a orbitals move only in the xy plane, the AF structure is stabilized in each xy plane independently due to superexchange interaction, as schematically shown in Fig. 7(c). On the other hand, the electrons in Γ_8^b orbitals can move itinerantly within the network composed of Γ_8^b orbitals due to the existence of holes in Γ_8^b orbitals. Since the hopping amplitude along the z axis is dominant in the region near $t_z=1$, the motion of Γ_8^b electrons causes an FM spin arrangement of Γ_8^a electrons along the z axis to gain kinetic energy. Namely, even though localized t_{2g} spins do not exist in the present case, the so-called double-exchange mechanism is always active in the two-orbital model. Note that the C-AF structure disappears for large Δ, since all the electrons tend to occupy Γ_8^a orbitals and the double-exchange mechanism is no longer active in that situation.
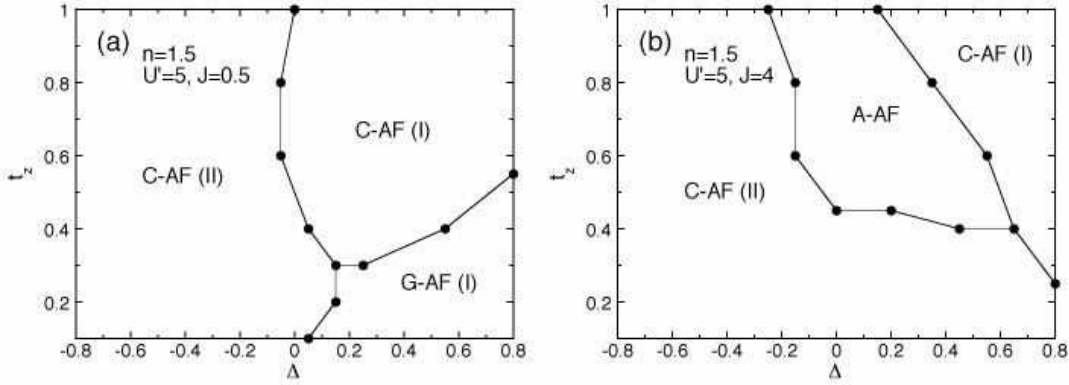
Figure 8. Ground-state phase diagram of the magnetic structure in the (Δ, t_z) plane for $n=1.5$, $U'=5$, (a) $J=0.5$ and (b) $J=4$.

After calculations of the spin and orbital correlations for several parameter sets, we obtain the ground-state phase diagram in the (Δ, t_z) plane, as shown in Fig. 7(d). It is found that the C-AF(I) phase discussed above extends to a wide region of $t_z<1$ in the phase diagram. Note that for small values of t_z, another C-AF phase, which we call C-AF(II), appears in the region of negative small Δ, in which the spin correlations of $(\pi, 0, \pi)$ and $(0, \pi, \pi)$ are dominant. For small t_z and large negative Δ, there appears yet another G-AF phase, called G-AF(III), due to the same reason as that for the occurrence of G-AF(I) phase for positive Δ, but the occupied orbital is changed from Γ_8^a to Γ_8^b. In any case, for $J=0$, we can observe several kinds of C- and G-AF phases, but A-AF phase does not occur.

Although we increase the value of J as $J=0.5$, no new phases appear in the phase diagram for $n=1.5$, as shown in Fig. 8(a). There are three phases, but they are two C-AF and one G-AF states. As labelled explicitly in the phase diagrams, C-AF(I), C-AF(II), and G-AF(I) are the same as those in the phase diagram of Fig. 7(d). Due to the effect of J, G-AF(II) and G-AF(III) disappear, since the number of FM bonds should be increased to gain the kinetic energy. As shown in Fig. 8(b), when we further increase the value of J as $J=4$, the G-AF phase completely disappears and instead, we observe the A-AF phase sandwiched by two C-AF phases. As described above, due to the double-exchange mechanism in the two-orbital model, the A-AF phase is considered to appear, when J is increased.

4. Discussion and Summary

In this paper, we have proposed an effective model with active orbital degree of freedom to understand the magnetic structure of neptunium 115 compounds from the microscopic viewpoint. By analyzing the model with the use of the exact diagonalization technique, we have obtained the ground-state phase diagrams including three kinds of AF phases corresponding to $NpTGa_5$.

In the experiments for NpTGa$_5$, C-, A-, and G-AF magnetic phases have been found in NpFeGa$_5$, NpCoGa$_5$, and NpNiGa$_5$. Here we have a question: What is a key parameter to understand the change of the magnetic structure? In the case of UTGa$_5$, it has been claimed that the level splitting Δ is important to explain the difference in magnetic structure as well as the magnetic anisotropy for a fixed value of $n=1$ [57]. Roughly speaking, Δ is positive for T=Fe, small positive for T=Co, and negative for T=Ni. Among UTGa$_5$ with T=Ni, Pd, and Pt, when we assume that the absolute value of Δ is increased in the order of Ni, Pd, and Pt, it is possible to understand qualitatively the change in the magnetic anisotropy, in addition to the change in the magnetic structure of G-AF for T=Ni and A-AF for T=Pd and Pt. It has been found that the value of t_z is not so crucial to explain qualitatively the magnetic properties of U-115 based on the two-orbital model for $n=1$.

For $n=2$, as emphasized in the previous section, we always obtain the G-AF phase. However, for $n=1.5$, we have observed three kinds of AF magnetic structure in the phase diagrams. Let us summarize the change in the magnetic structure for a fixed value of $t_z=0.8$. Note that this value is larger than $t_z=0.1$, which we have considered to reproduce two kinds of cylindrical Fermi-surface sheets of Np-115. However, in the small-sized cluster calculations, it is difficult to compare directly with the values in the thermodynamic limit. Thus, we do not discuss further the quantitative point on the values of t_z here. As shown in Fig. 7(d), for $J=0$ and $t_z=0.8$, we see the change in the magnetic structure as G-AF ($\Delta<0$), C-AF($0<\Delta<0.4$), and G-AF ($\Delta>0.4$). For $J=0.5$ and $t_z=0.8$, as shown in Fig. 8(a), the C-AF phases are always observed, but they have different orbital structures. Finally, for $J=4$ and $t_z=0.8$, we observe C-AF ($\Delta<-0.15$), A-AF($-0.15<\Delta<0.3$), and C-AF ($\Delta>0.3$), as shown in Fig. 8(b).

In order to understand the appearance of three types of the AF phases, we may consider an explanation due to the combination of the changes in Δ and n. For instance, by assuming that $J=4$ for NpTGa$_5$ and the change in Δ for NpTGa$_5$ is just the same as that for UTGa$_5$, we consider that $n\approx2$ with $\Delta<0$ for T=Ni, $n\approx1.5$ with $\Delta\approx0$ for T=Co, and $n\approx1.5$ with $\Delta>0$ for T=Fe. Then, it seems to be possible to relate our theoretical AF phases with the experimental observations in NpTGa$_5$. However, it is difficult to claim that the above parameter assignment for three Np-115 materials is the best explanation for the magnetic structure of Np-115, since in actual compounds, there are other important ingredients which have not been included in the present model. For instance, we have never discussed the direction of the magnetic moment of Np ion. Especially, the canted AF structure cannot be considered at all for the G-AF phase of NpNiGa$_5$. Thus, we need to recognize some distance between the actual magnetic states and the theoretically obtained phases. Our theory should be improved by taking into account other ingredients of 115 structure.

In summary, we have analyzed the orbital degenerate model appropriate for NpTGa$_5$ by using the exact diagonalization technique. Our phase diagram includes C-, A-, and G-AF phases. We have proposed the manganite-like scenario to understand the appearance of three kinds of AF spin structure in Np-115. Namely, the double-exchange

mechanism works also in some actinide compounds based on the model with active orbital degree of freedom. We believe that the present model can grasp some important points of the actinide compound by regarding it as charge-spin-orbital complex.

Acknowledgement

References

[1] E. Dagotto, T. Hotta, and A. Moreo, Phys. Rep. **344**, 1 (2001). See also E. Dagotto, *Nanoscale Phase Separation and Colossal Magnetoresistance*, Springer-Verlag, Berlin, 2002.

[2] See, for instance, *Colossal Magnetoresistance Oxides*, edited by Y. Tokura, Gordon & Breach, New York, 2000.

[3] A. Muñoz, M. T. Casáis, J. A. Alonso, M. J. Martínez-Lope, J. L. Martínez, and M. T. Fernández-Díaz, Inorg. Chem. **40**, 1020 (2001).

[4] T. Kimura, S. Ishihara, K. T. Takahashi, H. Shintani, and Y. Tokura, Phys. Rev. B **68**, 060403 (2003).

[5] E. O. Wollan and W. C. Koehler, Phys. Rev. **100**, 545 (1955).

[6] T. Hotta, M. Moraghebi, A. Feiguin, A. Moreo, S. Yunoki, and E. Dagotto, Phys. Rev. Lett. **90**, 247203 (2003).

[7] T. Hotta, Y. Takada, and H. Koizumi, Int. J. Mod. Phys. B **12**, 3437 (1998).

[8] T. Hotta, Y. Takada, H. Koizumi, and E. Dagotto, Phys. Rev. Lett. **84**, 2477 (2000).

[9] T. Hotta, A. L. Malvezzi, and Elbio Dagotto, Phys. Rev. **B62**, 9532 (2000).

[10] T. Mizokawa and A. Fujimori, Phys. Rev. B**51**, 12880 (1995); **54**, 5368 (1996).

[11] I. Solovyev, N. Hamada, and K. Terakura, Phys. Rev. Lett. **76**, 4825 (1996); Phys. Rev. B**53**, 7158 (1996).

[12] W. Koshibae, Y. Kawamura, S. Ishihara, S. Okamoto, J. Inoue, and S. Maekawa, J. Phys. Soc. Jpn. **66**, 957 (1997).

[13] R. Shiina, T. Nishitani, and H. Shiba, J. Phys. Soc. Jpn. **66**, 3159 (1997).

[14] S. Ishihara, J. Inoue, and S. Maekawa, Phys. Rev. B**55**, 8280 (1997).

[15] H. Sawada, Y. Morikawa, K. Terakura, and N. Hamada, Phys. Rev. B**56**, 12154 (1997).

[16] D. Feinberg, P. Germain, M. Grilli, and G. Seibold, Phys. Rev. B**57**, R5583 (1998).

[17] R. Maezono, S. Ishihara, and N. Nagaosa, Phys. Rev. B**57**, R13993 (1998).

[18] L. F. Feiner and A. M. Oleś, Phys. Rev. B**59**, 3295 (1999).

[19] P. Horsch, J. Jaklič, and F. Mack, Phys. Rev. B**59**, 6217 (1999).

[20] J. van den Brink, P. Horsch, F. Mack, and A. M. Oleś, Phys. Rev. B**59**, 6795 (1999).

[21] P. Benedetti and R. Zeyher, Phys. Rev. B**59**, 9923 (1999).

[22] T. Hotta, S. Yunoki, M. Mayr, and E. Dagotto, Phys. Rev. B**60**, R15009 (1999).

[23] P. B. Allen and V. Perebeinos, Phys. Rev. B**60**, 10747 (1999).

[24] M. Capone, D. Feinberg, and M. Grilli, Euro. Phys. J. B**17**, 103 (2000).

[25] J. C. Loudon, N. D. Mathur, and P. A. Midgley, Nature (London) **420**, 797 (2002).

[26] N. D. Mathur and P. Littlewood, Physics Today **56**, 25 (2003).

[27] S. Yunoki, T. Hotta, and E. Dagotto, Phys. Rev. Lett. **84**, 3714 (2000).

[28] T. Hotta, A. Feiguin, and E. Dagotto, Phys. Rev. Lett. **86**, 4922 (2001).

[29] T. Hotta and E. Dagotto, Phys. Rev. Lett. **88**, 017201 (2002).

[30] F. Nakamura, T. Goko, M. Ito, T. Fujita, S. Nakatsuji, H. Fukazawa, Y. Maeno, P. Alireza, D. Forsythe, and S. R. Julian, Phys. Rev. B**65**, 220402(R) (2002).

[31] T. Hotta and E. Dagotto, Phys. Rev. Lett. **92**, 227201 (2004).

[32] J. L. Sarrao, L. A. Morales, J. D. Thompson, B. L. Scott, G. R. Stewart, F. Wastin, J. Rebizant, P. Boulet, E. Colineau, and G. H. Lander, Nature (London) **420**, 297 (2002).

[33] J. L. Sarrao, J. D. Thompson, N. O. Moreno, L. A. Morales, F. Wastin, J. Rebizant, P. Boulet, E. Colineau, and G. H. Lander, J. Phys.: Condens. Matter **15**, S2275 (2003).

[34] F. Wastin. P. Boulet, J. Rebizant, E. Colineau, and G. H. Lander, J. Phys.: Condens. Matter **15**, S2279 (2003).

[35] T. Hotta and K. Ueda, Phys. Rev. B**67**, 104518 (2003).

[36] T. Maehira, T. Hotta, K. Ueda, and A. Hasegawa, Phys. Rev. Lett. **90**, 207007 (2003).

[37] Y. N. Grin, P. Rogl, and K. Hiebl, J. Less-Common Met. **121**, 497 (1986).

[38] V. Sechovský, L. Havela, G. Schaudy, G. Hilscher, N. Pillmayr, P. Rogl, and P. Fischer, J. Magn. Magn. Mater. **104-107**, 11 (1992).

[39] S. Noguchi and K. Okuda, J. Magn. Magn. Mater. **104-107**, 57 (1992).

[40] K. Okuda and S. Noguchi, in *Physical Properties of Actinide and Rare Earth Compounds*, edited by T. Kasuya, T. Ishii, T. Komatsubara, S. Sakai, N. Môri, and T. Saso, JJAP Series 8 (Publication Office, JJAP, Tokyo, 1993), p. 32.

[41] Y. Ōnuki, D. Aoki, P. Wiśnieski, H. Shishido, S. Ikeda, Y. Inada, R. Settai, Y. Tokiwa, E. Yamamoto, Y. Haga, T. Maehira, H. Harima, M. Higuchi, A. Hasegwa, and H. Yamagami, Acta Phys. Pol. B**32**, 3273 (2001).

[42] Y. Tokiwa, Y. Haga, E. Yamamoto, D. Aoki, N. Watanabe, R. Settai, T. Inoue, K. Kindo, H. Harima, and Y. Ōnuki, J. Phys. Soc. Jpn. **70**, 1744 (2001).

[43] Y. Tokiwa, T. Maehira, S. Ikeda, Y. Haga, E. Yamamoto, A. Nakamura, Y. Ōnuki, M. Higuchi, and A. Hasegawa, J. Phys. Soc. Jpn. **70**, 2982 (2001).

[44] Y. Tokiwa, Y. Haga, N. Metoki, Y. Ishii, and Y. Ōnuki, J. Phys. Soc. Jpn. **71**, 725 (2002).

[45] Y. Tokiwa, S. Ikeda, Y. Haga, T. Ōkubo, T. Iizuka, K. Sugiyama, A. Nakamura, Y. Ōnuki, J. Phys. Soc. Jpn. **71**, 845 (2002).

[46] H. Kato, H. Sakai, Y. Tokiwa, S. Kambe, R. E. Walstedt, and Y. Ōnuki, J. Phys. Chem. Solids **63**, 1197 (2002).

[47] S. Ikeda, Y. Tokiwa, Y. Haga, E. Yamamoto, T. Ōkubo, M. Yamada, N. Nakamura, K. Sugiyama, K. Kindo, Y. Inada, H. Yamagami, and Y. Ōnuki, J. Phys. Soc. Jpn. **72**, 576 (2003).

[48] K. Kaneko, N. Metoki, N. Bernhoeft, G. H. Lander, Y. Ishii, S. Ikeda, Y. Tokiwa, Y. Haga, and Y. Ōnuki, Phys. Rev. B **68**, 214419 (2003).

[49] E. Colineau, P. Javorský, P. Boulet, F. Wastin, J. C. Griveau, J. Rebizant, J. P. Sanchez, and G. R. Stewart, Phys. Rev. B **69**, 184411 (2004).

[50] D. Aoki, E. Yamamoto, Y. Homma, Y. Shiokawa, A. Nakamura, Y. Haga, R. Settai, and Y. Ōnuki, J. Phys. Soc. Jpn. **73**, 519 (2004).

[51] D. Aoki, Y. Homma, Y. Shiokawa, E. Yamamoto, A. Nakamura, Y. Haga, R. Settai, T. Takeuchi, and Y. Ōnuki, J. Phys. Soc. Jpn. **73**, 1665 (2004).

[52] D. Aoki, Y. Homma, Y. Shiokawa, E. Yamamoto, A. Nakamura, Y. Haga, R. Settai, and Y. Ōnuki, J. Phys. Soc. Jpn. **73**, 2608 (2004).

[53] F. Honda, N. Metoki, K. Kaneko, D. Aoki, Y. Homma, E. Yamamoto, Y. Shiokawa, Y.Ōnuki, E. Colineau, N. Bernhoft, and G. H. Lander, submitted to Physica B (Proceedings of SCES2004).

[54] E. Yamamoto, D. Aoki, Y. Homma, Y. Shiokawa, Y. Haga, A. Nakamura, and Y. Ōnuki, submitted

to Physica B (Proceedings of SCES2004).

[55] Y. Homma, S. Nasu, D. Aoki, K. Kaneko, N. Metoki, E. Yamamoto, A. Nakamura, S. Morimoto, H. Yasuoka, Y. Ōnuki, and Y. Shiokawa, submitted to Physica B (Proceedings of SCES2004).

[56] N. Metoki *et al.*, preprint.

[57] T. Hotta, Phys. Rev. B **70**, 054405 (2004).

[58] W. Knafo, S. Raymond, B. Fak, G. Lapertot, P. C. Canfield, and J. Flouquet, J. Phys.: Condens. Matter **15**, 3741 (2003).

[59] G. Zwicknagl and P. Fulde, J. Phys.: Condens. Matter **15**, S1911 (2003).

[60] D. V. Efremov, N. Hasselmann, E. Runge, P. Fulde, and G. Zwicknagl, Phys. Rev. B **69**, 115114 (2004).

[61] E. Runge, P. Fulde, D. V. Efremov, N. Hasselmann, and G. Zwicknagl, Phys. Rev. B **69**, 155110 (2004).

[62] K. Kubo and T. Hotta, cond-mat/0409116.

[63] T. Hotta and K. Ueda, Acta Phys. Pol. B **34**, 443 (2003).

[64] E. Colineau, F. Wastin, P. Boulet, P. Javorský, and J. Rebizant, submitted to Physica B (Proceedings of SCES2004).

[65] P. Boulet, E. Colineau, F. Wastin, P. Javorský, and J. Rebizant, submitted to Physica B (Proceedings of SCES2004).

[66] E. Colineau, F. Bourdarot, P. Burlet, J. P. Sanchez, and J. Larroque, Physica B **230-232**, 773 (1997).